SINGLE IMAGE SUPER-RESOLUTION USING SPARSE REPRESENTATIONS WITH STRUCTURE CONSTRAINTS

J. C. Ferreira[∗†⋆] *O. Le Meur*[†] *C. Guillemot*[†] *E. A. B. da Silva*[◊] *G. A. Carrijo*[⋆]

[†] SIROCCO Research team, INRIA, France
[◊]COPPE, Federal University of Rio de Janeiro - UFRJ, Brazil
[⋆]FEELT, Federal University of Uberlândia - UFU, Brazil

ABSTRACT

This paper describes a new single-image super-resolution algorithm based on sparse representations with image structure constraints. A structure tensor based regularization is introduced in the sparse approximation in order to improve the sharpness of edges. The new formulation allows reducing the ringing artefacts which can be observed around edges reconstructed by existing methods. The proposed method, named Sharper Edges based Adaptive Sparse Domain Selection (SE-ASDS), achieves much better results than many state-of-the-art algorithms, showing significant improvements in terms of PSNR (average of 29.63, previously 29.19), SSIM (average of 0.8559, previously 0.8471) and visual quality perception.

Index Terms: super-resolution, sparse representations, structure tensors.

1. INTRODUCTION

Single-image super-resolution refers to the problem of generating a high-resolution (HR) output image, given one low-resolution (LR) image as an input. The super-resolution (SR) task is an ill-conditioned inverse problem solved as there can be several HR images generating the same LR image. The problem is usually solved by exploiting observation and *a priori* image models with regularization techniques. The single-image SR methods can be broadly classified into two categories: interpolation-based methods often exploiting statistical image priors [1], [2], [3]; and learning-based methods which use a dictionary of learned co-occurrence priors between LR and HR patches to estimate the HR image [4], [5], [6]. The learning methods which make use of patches are also referred to as Example-based SR [6].

The method described in Dong et al. [7], called Adaptive Sparse Domain Selection scheme (ASDS), is a mixed approach based on the sparse association between input and example patches stored in a union of adaptively selected dictionaries. The locally sparse association is further constrained by additional image priors introduced as two adaptive regularization terms. The first regularization term uses autoregressive (AR) models learned from the training set image patches whereas the second regularization term introduces a constraint in terms of non-local self similarity. Although the method in [7] already performs well, it does not take into account geometric image structures, hence still suffers from artefacts around edges.

Here, we describe a new single-image SR algorithm built upon the idea of adaptive sparse domain selection exploiting regulation constraints driven by the image geometrical structure. In order to do so, a new structure tensor-based regularization term is introduced in the sparse approximation formulation in order to obtain sharper edges. This new regularization term is specifically applied on edges of the reconstructed image. Therefore, this algorithm is named sharper edges based ASDS (SE-ASDS). Experimental results on a large set of test images show that the proposed method brings significant improvements both in terms of PSNR, SSIM and visual quality, compared to various state of the art methods.

2. SUPER-RESOLUTION USING SPARSE REPRESENTATIONS: BACKGROUND

Sparsity has been used in different single-image SR algorithms, particularly in learning-based methods.

In [5], Yang et al. aim to recover an image I_h from its respective image I_l using the constraint that the estimated $\hat{I}_h$ image should yield I_l images when the model $I_l = LI_h$ is applied. Patches of the I_h can be represented as a sparse linear combination of atoms extracted from a dictionary D_h. This dictionary has been trained off-line from high resolution patches sampled from training images $x \approx D_h\alpha$, where α is a sparse vector of weights. The method proposed by [5] outperforms [4], [1] and [2] when applied either on noisy or noiseless images.

In [8], Kulkarni et al. make a parallel between sparse representations using dictionaries and sparse representations using orthonormal bases. Experiments show that sparse representations is satisfied for several kinds of dictionaries, such as learned dictionaries and non-trained dictionary [8]. However, Kulkarani et al. give evidences that trained dictionaries perform much better than non-trained dictionaries in terms of consistency for solutions, local patchwise discontinuities and performance.

In [7], Dong et al. proposes a non-blind algorithm with adaptive sparse domain selection (ASDS) using sparse representation. It aims at recovering a high resolution image I_h from its I_l using a set of pre-learned compact dictionaries from high quality images trained using principal component analysis (PCA). The main idea of this method is to choose the best trained dictionary for each patch. Besides, Dong et al. use sparse representations to solve the inverse problem of SR, assuming that the estimated image is sparse in the selected domain. In addition to sparsity-based regularization, two complementary regularization terms are used: one explores the local image structures thanks to auto-regressive models (AR) whereas the other one uses the non-local redundancy to enhance each local path (NL).

Given a low resolution image I_l, Dong et al. want to recover $\hat{I}_h$ using the following minimization problem:

$$\hat{I}_h = \arg\min_{I_h} E\left(I_h\right) \tag{1}$$

[∗]The first author would like to thank CAPES Brazilian agency for the financial support (PDSE scholarship 18385-12-5).

Fig. 1: Results generated using Dong et al.'s code [7]. There are some ringing noise around edges in the three images.

The cost function $E(I_h)$, used to stabilize the solution of this ill-posed inverse problem, is given by

$$E(I_h) = E(I_h\,|I_l) + E_{AR}(I_h) + E_{NL}(I_h) + E_\alpha(I_h) \quad (2)$$

where the first term $E(I_h\,|I_l)$ is the fidelity term whereas the three others are regularization terms. The term $E_{AR}(I_h)$ is based on estimated local structure, $E_{NL}(I_h)$ exploits the non-local similarity and $E_\alpha(I_h)$ is the sparsity penalty term. Dong et al. present an iterative shrinkage algorithm to solve the l_1-minimization problem presented in Equation (1).

In their paper, Dong et al. [7] have noted that Daubechies et al. [9] generate results with many jaggy and ringing artifacts; Marquina et al. [10] present results with piece-wise constant block artifacts although their method is effective in suppressing the ringing; Dai et al. [11] produce artificial images due to very smooth edges and fine structures. The method of Yang et al. [12] performs quite well. However, two universal dictionaries are required to get the result. In addition, the reconstructed edges are relatively smooth and some fine image structures are not well (or at all) recovered. Besides, the authors observe that methods [9],[10], [12] are sensitive to noise and generate artifacts around edges. Thus, Dong et al. [7] generate better results in terms of PSNR, SSIM and visual quality than the aforementioned methods for noiseless and noisy images. In Dong et al., the edges are much sharper than all the other methods with however some ringing noise around edges as illustrated in figure 1.

Considering that the original scenario of Dong et al.'s method produces some ringing artifacts around the reconstructed edges, we believe that the method can be improved in terms of PSNR, SSIM and visual quality. With this aim, we introduce a new regularization term which is based on structure tensors in order to improve the sharpness of edges.

Before describing this new regularization term, the following section elaborates on the computation of structure tensors which are used to estimate the local geometry of images.

3. REGULARIZATION BASED ON STRUCTURE TENSORS

Let $\Omega \rightarrow \mathcal{Z}^2$ with $(x, y) \in \Omega$ and let $I : \Omega \rightarrow \mathcal{R}^3$ be a vector-valued data set and I_j its j-th channel. The tensor structure $\mathbf{J}$, also called Di Zenzo matrix [13], is given by

$$\mathbf{J} = \sum_{j=1}^{n} \nabla I_j \nabla I_j^T \quad (3)$$

where $\mathbf{J}$ is the sum of the scalar structure tensors $\nabla I_j \nabla I_j^T$ of each image channel I_j and ∇I_j refers to the gradient.

In this work, we use the luma-channel Y of the YCbCr image, i.e., $j = 1$ in Equation (3). The partial derivatives in x and y directions are obtained by applying the rotational symmetric filter proposed in [14]. Most of the time, the structure tensor $\mathbf{J}$ is locally smoothed with a Gaussian kernel in order to reduce the influence of noise and to strengthen its coherence. However, being isotropic and linear, this regularization may significantly alter the local structure of the image [15] by over-smoothing corners. To overcome this problem, a non-linear anisotropic regularization is performed. Doré et al. [15] recently extended the non local filter to regularize structure tensors. The main drawback of this approach is its complexity.

Instead of using the aforementioned methods, the regularization of $\mathbf{J}$ is achieved by using a simple Difference of Gaussians filter introduced in [16]. They are assigned to the regularization of each component of the tensor $\mathbf{J}$. We note $\mathbf{J}_r$ the result of the regularization.

From the spectral decomposition, this structure tensor can be rewritten as

$$\mathbf{J}_r = \lambda_+ \theta_+ \theta_+^T + \lambda_- \theta_- \theta_-^T \quad (4)$$

where $\lambda_\pm$ are the eigenvalues and $\theta_\pm$ are the eigenvectors (or the components of an orthonormal vector basis in $\mathcal{R}^2$). The eigenvalues show the strength of the local image edges and the eigenvectors θ_+, associated to the highest eigenvalues λ_+, define the direction of the highest change normal to the edges.

The regularized structure tensor is shown in the following equation

$$\mathbf{J}_r = \begin{bmatrix} g_{11} & g_{12} \\ g_{12} & g_{22} \end{bmatrix} = \begin{bmatrix} \left(\nabla I_x \nabla I_x^T\right) & \left(\nabla I_x \nabla I_y^T\right) \\ \left(\nabla I_x \nabla I_y^T\right) & \left(\nabla I_y \nabla I_y^T\right) \end{bmatrix} * G^{4\sigma} \quad (5)$$

where ∇I_x and ∇I_y are computed using separable Gaussian derivative kernels DoG_x^σ and DoG_y^σ on the channel I_j of the image I, G is a Gaussian kernel and $(*)$ is the convolution operation.

The eigenvalues is given by

$$\lambda_\pm = \frac{g_{11} + g_{22} \pm \sqrt{(g_{11} - g_{22})^2 + 4g_{12}^2}}{2} \quad (6)$$

and the eigenvectors is given by

$$\theta_\pm = \begin{bmatrix} 2g_{12} \\ g_{22} - g_{11} \pm \sqrt{(g_{11} - g_{22})^2 + 4g_{12}^2} \end{bmatrix} \quad (7)$$

The relative discrepancy between the two eigenvalues of $\mathbf{J}_r$ is an indicator of the degree of anisotropy of the gradient in a region of the image. A coherence measure is often given by $(\frac{\lambda_+ - \lambda_-}{\lambda_+ + \lambda_-})^2$ [17]. However, it is known that the coherence measure fails to detect saddle points (i.e. when $\lambda_+ \approx \lambda_- \approx 0$) [18]. In order to detect salient edges, we use the function named as S-norm presented in Equation (8), where $p = (x, y)$ represent the pixel coordinates.

$$S(p) = \frac{\lambda_+(p)}{\max_{p \in I} \lambda_+(p)} \quad (8)$$

In the next section, we characterize the proposed regularization term named here the edgeness term.

3.1. Edgeness term

The edgeness term is the heart of the proposed SE-ASDS method. Considering that the eigenvector θ_+ indicates the direction normal to the edges, we start from the current pixel p belonging to the edge, named as p_{sl}^0, and we trace a stream line of size $2sl + 1$ as illustrated in Figure 2.

The energy term $E_{Edg}(I_h)$ is used to enhance the sharpness of the current location. It is given by the following equation

$$E_{Edg}(I_h) = \phi(p) \frac{\beta_2}{2} \left(I_h(p) - \tilde{I_h}^{edg}(p) \right)^2 \quad (9)$$

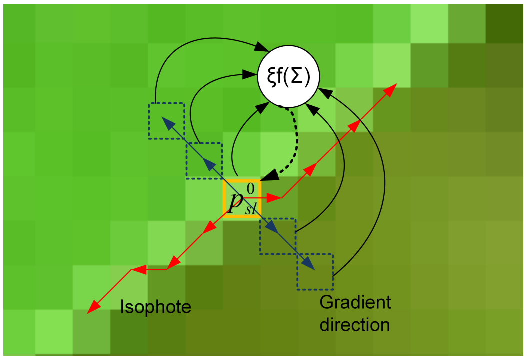

Fig. 2: The yellow box corresponds to the current pixel p_{sl}^0. The stream line is given in blue; The energy term E_{Edg} forces the value of the current pixel to be as close as possible to pixel values having lowest saliency (i.e., meaning that pixel belongs to flat area).

where β_2 is a regularization parameter and $\phi(p)$ allows to apply this constraint only on salient edges.

For a spatial located pixel p, the function ϕ is given by

$$\phi(p) = \begin{cases} 1, & S(p) > \nu \\ 0, & otherwise \end{cases} \tag{10}$$

with ν a constant threshold and $S(p)$ is defined by Equation (8).

In Equation (9), $\tilde{I_h}^{edg}$ is the linear combination of pixel values of the stream line in the direction $\pm\theta_+$, defined by

$$\tilde{I_h}^{edg} = \sum_{i=-sl}^{sl} \alpha_i I^h(p_{sl}^i) \tag{11}$$

where p_{sl}^i are the pixels values located on the stream line defined by direction $\pm\theta_+$ in p_{sl}^0. The weights α_i are computed as

$$\alpha_i = \xi_i \exp\left(-\frac{\left[I_h(p_{sl}^i) - I_h(p_{sl}^0)\right]^2}{h}\right) \tag{12}$$

where $\left[I_h(p_{sl}^i) - I_h(p_{sl}^0)\right]^2$ is squared difference between the pixel $I_h(p_{sl}^i)$ belonging to the stream line and the central pixel p_{sl}^0; and h is a decay factor. In this work, h is adaptively computed as the instantaneous power $h = \|.\|_2$ for each stream line. Weights α_i are positive and normalized such that $\sum_{i=-sl}^{sl} \alpha_i = 1$.

The weights $\{\xi_i\}$ are binary and computed using the following equation:

$$\xi(p_{sl}^i) = \begin{cases} 1, & S(p_{sl}^i) \leq S(p_{sl}^0) \\ 0, & otherwise \end{cases} \tag{13}$$

The main idea is to sharpen salient edges by forcing the current pixel value to be as close as possible to values of pixels belonging to less salient edges. The next section presents the new regularization term $E_{Edg}(I_h)$.

3.2. Minimization

The proposed method minimizes the cost function

$$E(I_h) = E(I_h\,|I_l) + E_{Edg}(I_h) + E_{NL}(I_h) + E_\alpha(I_h) \tag{14}$$

where the term $E_{Edg}(I_h)$ denotes the new edgeness term which is used instead of the $E_{AR}(I_h)$ regularization term in Equation (2).

The minimization of energy in Equation (14) is achieved by using the same Iterative Shrinkage Thresholding (IST) as Dong et al. [7]. The starting point of this iterative scheme is given by a first HR guess noted I_h^0:

$$I_h^{t+1} = I_h^t - \frac{\partial E(I_h^t)}{\partial I_h} \tag{15}$$

where

$$\begin{aligned} \frac{\partial E(I_h^t)}{\partial I_h} \approx \quad & \beta_1\left((I_h * G)\downarrow - I_l\right)\uparrow * G \\ & + \beta_2\phi(p)\left(I_h - I_h^{edg}\right) \\ & + \beta_3\left(I_h - I_h^{NL}\right) \\ & + \beta_4\,|\alpha|_1 \end{aligned} \tag{16}$$

and α is a sparse representation of I_h on a sub-dictionary Φ_k trained by Dong et al. [7].

Note that Equation (16) is an approximation since the derivative of the new edgeness term $\frac{\partial E_{Edg}(I_h)}{\partial I_h}$ is not rigorously equal to $\beta_2\phi(p)\left(I_h - I_h^{edg}\right)$. In order to derive the second term of Equation (16) (second line), we made the assumption that $I_h(p_{sl}^i) \approx I_h(p_{sl}^0)$ in Equation (12). To the best of our knowledge, this strategy is reasonable and locally valid when we choose a short length stream line as in performed experiments.

In the next section, we present a simple algorithm to compute the sharper image and, consequently, the edgeness term.

3.3. Implementation

The pseudo-code of the proposed algorithm for computing the edgeness term is described in Algorithm 1.

Algorithm 1: Implementation of the I_h^{edg} for SE-ASDS

input : HR image I_h^0; iterations N; constant ζ.
output: sharper HR image I_h^{edg}.
for $i \leftarrow 0$ **to** N **do**
  Compute the structure tensor $\mathbf{J}$;
  Compute the regularized structure tensor $\mathbf{J}_r$;
  Compute eigenvectors and eigenvalues;
  Compute the energy term $E = \frac{\partial E_{Edg}(I_h)}{\partial I_h}$;
  foreach *pixel p of the HR picture* **do**
    $I_h^{i+1}(p) = I_h^i(p) - \zeta E(p)$

The structure tensor is computed using smooth derivatives on the current estimated HR picture leading to a set of eigenvalues and eigenvectors. These eigenvalues and eigenvectors are used to compute a stream line for each pixel p belonging to the edge. Then, only the values of p that are salient are changed. The energy term dealing with the sharpness of edges is computed and used to modify the current estimated HR picture inside the IST algorithm [7]. As the the algorithm changes the value of the pixel p each time, we iterate the Algorithm 1. Finally, a sharper image I_h^{edg} is computed and can be used to regularize Equation (16) [7].

Several experiments are conducted and presented in the next section.

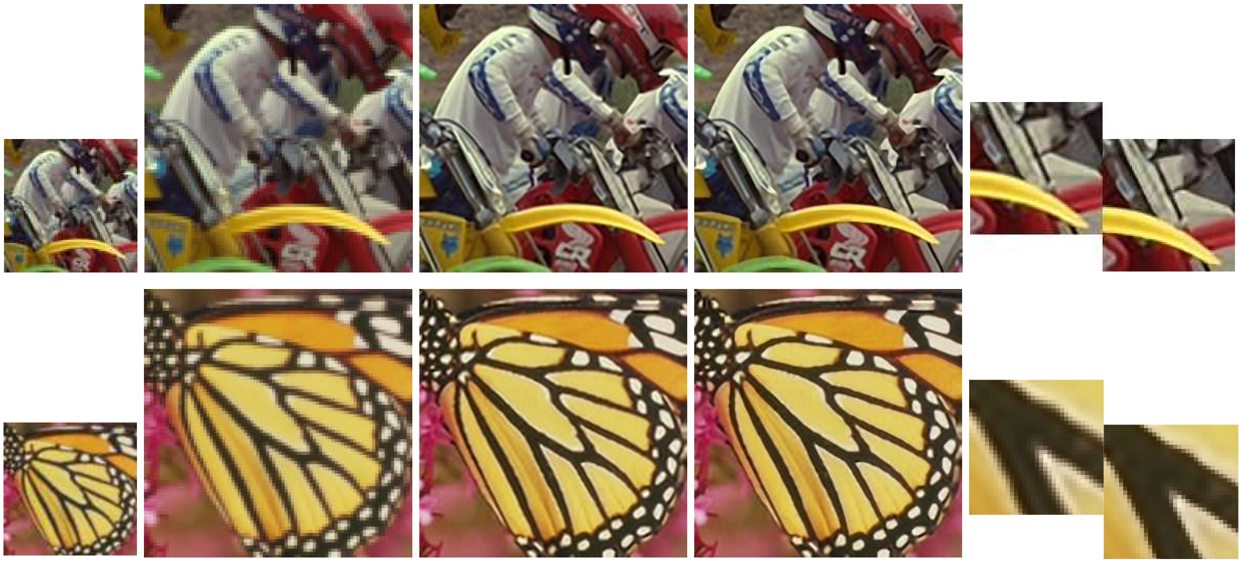

(a) 86 × 86 (b) Nearest (c) Dong et al.'s ASDS (d) SE-ASDS (e) Zoom between (c) and (d)

Fig. 3: Comparison of SR results (×3). (a) LR image;(b) Nearest-neighbor; (c) Dong et al.'s ASDS results: images are still blurry and edges are not sharp. (d) SE-ASDS results: better results. (e) Comparison between (c) and (d) on patches: edges of (d) are more contrasted than (c).

4. EXPERIMENTAL RESULTS

In our experiments, I_l were obtained by applying a 7 × 7 Gaussian kernel filter of standard deviation 1.6 on the same benchmark images used by Dong et al. [7] and then sub-sampling by a factor 3. The same IST algorithm and trained previous dictionaries by Dong et al. were used. The method is only applied on the luminance Y channel and the color channels are up-sampled using bi-cubic interpolation. The up-sampling factor is of 3. The parameters β_1, β_3 and β_4 are selected as Dong et al. and β_2 is set to 0.009.

To compute the edgeness term I_h^{edg}, we set $\nu = 0.01$, $\zeta = 0.05$, $N = 2$ iterations and the total length of the stream lines equal to 7 pixels, i.e. $sl = 3$. Since the function ξ controls the weights taking into consideration the value of $S(p)$, different short lengths of stream lines can be set obtaining similar results.

We compare the proposed approach with [9], [12], [11], [10], and with the best results obtained by Dong et al. [7]. In [9], Daubechies et al. consider linear inverse problems where the solution is presupposed to have a sparse expansion on an arbitrary orthonormal basis. In [11], Dai et al. propose a technique based on edge smoothness prior to suppress the jagged edge artifact. In [10], Marquina and Osher present a super-resolution algorithm based on a constrained variational model that uses the total variation as a regularization term.

Figure 3 illustrates the results obtained by the proposed SE-ASDS method and by two other methods. Among these approaches, the best results are given by SE-ASDS method as demonstrated by Figure 3 (e) and the last column of Table 1. Results are less blurry and more sharpen than other solutions. The same behavior was obtained when we add a gaussian noise to the images with a standard deviation of 5. More results are available online[1].

[1] `http://people.irisa.fr/Olivier.Le_Meur/publi/2014_ICIP_Julio/`

Table 1: The PSNR (dB) and SSIM results (luminance components) of super-resolved HR images.

Images	[9]	[11]	[12]	[10]	[7]	SE-ASDS
Girl	32.93 0.8102	31.94 0.7704	32.51 0.7912	31.21 0.7878	33.54 0.8242	**33.56** **0.8252**
Parrot	28.78 0.8845	27.71 0.8682	27.98 0.8665	27.59 0.8856	30.00 0.9093	**30.29** **0.9136**
Butterfly	25.16 0.8336	25.19 0.8623	23.73 0.7942	26.60 0.9036	27.34 0.9047	**28.48** **0.9236**
Leaves	24.59 0.8310	24.34 0.8372	24.35 0.8170	24.58 0.8878	26.80 0.9058	**27.69** **0.9261**
Parthenon	26.32 0.7135	25.87 0.6791	24.08 0.6305	25.89 0.7163	26.83 0.7349	**27.05** **0.7446**
Flower	28.16 0.8120	27.50 0.7800	27.76 0.7929	27.38 0.8111	29.19 0.8480	**29.29** **0.8511**
Hat	29.92 0.8438	29.68 0.8389	29.65 0.8362	29.19 0.8569	30.93 0.8707	**31.53** **0.8805**
Raccoon	28.80 0.7549	27.96 0.6904	28.49 0.7273	27.53 0.7076	29.24 0.7677	**29.27** **0.7686**
Bike	23.48 0.7438	23.31 0.7219	23.20 0.7188	23.61 0.7567	24.62 0.7962	**24.97** **0.8098**
Plants	31.87 0.8792	31.45 0.8617	31.48 0.8698	31.28 0.8784	33.47 0.9095	**34.17** **0.9163**
Average	28.03 0.8115	27.49 0.7910	27.69 0.7954	27.49 0.8190	29.19 0.8471	**29.63** **0.8559**

5. CONCLUSION

The proposed SE-ASDS approach gives better results than Daubechies [9], Yang et al. [12], Dai et al. [11], Marquina and Osher [10] and Dong et al. [7] in terms of PNSR, SSIM and visual quality for all benchmark images. In our experiments, SE-ASDS is faster and gives in average 0.44 dB improvement compared to Dong et al.'s method in terms of PSNR. Other innovation was the use of h as instantaneous power of the stream line pixel values.

6. REFERENCES

[1] Michal Irani and Shmuel Peleg, "Motion analysis for image enhancement: resolution, occlusion, and transparency", *Journal of Visual Communication and Image Representation*, vol. 4, no. 4, pp. 324–335, Dec. 1993.

[2] Shengyang Dai, Mei Han, Wei Xu, Ying Wu, and Yihong Gong, "Soft edge smoothness prior for alpha channel super resolution", *2007 IEEE Conference on Computer Vision and Pattern Recognition*, pp. 1–8, June 2007.

[3] Raanan Fattal, "Image upsampling via imposed edge statistics", *ACM Transactions on Graphics (TOG)*, vol. 26, no. 3, 2007.

[4] Hong Chang, DY Yeung, and Yimin Xiong, "Super-resolution through neighbor embedding", in *Proceedings of the 2004 IEEE Computer Society Conference on Computer Vision and Pattern Recognition, 2004. CVPR 2004.* 2004, vol. 1, pp. 275–282, IEEE.

[5] Jianchao Yang, John Wright, Thomas Huang, and Yi Ma, "Image super-resolution via sparse representation.", *IEEE Transactions on Image Processing*, vol. 19, no. 11, pp. 2861–2873, Nov. 2010.

[6] W.T. Freeman, T.R. Jones, and E.C. Pasztor, "Example-based super-resolution", *IEEE Computer Graphics and Applications*, vol. 22, no. 2, pp. 56–65, 2002.

[7] Weisheng Dong, Lei Zhang, Guangming Shi, and Xiaolin Wu, "Image deblurring and super-resolution by adaptive sparse domain selection and adaptive regularization.", *IEEE Transactions on Image Processing*, vol. 20, no. 7, pp. 1838–57, July 2011.

[8] Naveen Kulkarni, Pradeep Nagesh, Rahul Gowda, and Baoxin Li, "Understanding compressive sensing and sparse representation-based super-resolution", *IEEE Transactions on Circuits and Systems for Video Technology*, vol. 22, no. 5, pp. 778–789, May 2012.

[9] Ingrid Daubechies, M. Defrise, and C. De Mol, "An iterative thresholding algorithm for linear inverse problems with a sparsity constraint", *Communications on Pure and Applied Mathematics*, vol. 57, no. 11, pp. 1413–1457, Nov. 2004.

[10] Antonio Marquina and Stanley J. Osher, "Image super-resolution by TV-regularization and bregman iteration", *Journal of Scientific Computing*, vol. 37, no. 3, pp. 367–382, July 2008.

[11] Shengyang Dai, Mei Han, Wei Xu, Ying Wu, Yihong Gong, and Aggelos K Katsaggelos, "SoftCuts: a soft edge smoothness prior for color image super-resolution.", *IEEE Transactions on Image Processing*, vol. 18, no. 5, pp. 969–81, May 2009.

[12] Jianchao Yang, John Wright, Thomas Huang, and Yi Ma, "Image super-resolution as sparse representation of raw image patches", in *2008 IEEE Conference on Computer Vision and Pattern Recognition*. June 2008, pp. 1–8, Ieee.

[13] Silvano Di Zenzo, "A note on the gradient of a multi-image", *Computer Vision, Graphics, and Image Processing*, vol. 33, no. 1, pp. 116–125, Jan. 1986.

[14] B Jähne, Hanno Scharr, and S Körkel, "Principles of filter design", *Handbook of computer vision and applications*, vol. 2, pp. 125–151, 1999.

[15] Vincent Doré, Reza Farrahi Moghaddam, and Mohamed Cheriet, "Non-local adaptive structure tensors", *Image and Vision Computing*, vol. 29, no. 11, pp. 730–743, Oct. 2011.

[16] D. Marr and E. Hildreth, "Theory of Edge Detection", *Proceedings of the Royal Society B: Biological Sciences*, vol. 207, no. 1167, pp. 187–217, Feb. 1980.

[17] Bernd Jähne, *Spatio-temporal image processing: theory and scientific applications*, vol. 751, Springer, 1993.

[18] Joachim Weickert, *Anisotropic diffusion in image processing*, ECMI Series. Teubner, Stuttgart, 1998.